Mitochondrial proteomic approach reveals galectin-7 as a novel BCL-2 binding protein in human cells

Christelle Villeneuve[a], Laurent Baricault[a], Ludovic Canelle[b], Nadia Barboule[a], Carine Racca[a], Bernard Monsarrat[b], Thierry Magnaldo[c], and Florence Larminat[a]
[a]LBCMCP, CNRS-UMR5088, and [b]IPBS, CNRS-UMR5089, Université de Toulouse, 31077 Toulouse, France; [c]LBPG, CNRS-UMR6267/INSERM U998, Faculté de Médecine, 06107 Nice, France

ABSTRACT **Although the anti-apoptotic activity of Bcl-2 has been extensively studied, its mode of action remains incompletely understood. Deciphering the network of Bcl-2 interacting factors is necessary to better understand the key function of Bcl-2 in apoptosis initiation. To identify novel Bcl-2 mitochondrial partners, we have combined a Bcl-2 immunocapture with a mass spectrometry analysis using highly pure mitochondrial fractions isolated from human cancer cells. We identified at high confidence 127 potential Bcl-2–interacting proteins. Gene ontology mining reveals enrichment for mitochondrial proteins, endoplasmic reticulum–associated proteins, and cytoskeleton-associated proteins. Importantly, we report the identification of galectin-7 (Gal7), a member of a family of β-galactoside–binding lectins that was already known to exhibit a pro-apoptotic function, as a new mitochondrial Bcl-2 interacting partner. Our data further show that endogenous Bcl-2 coimmunoprecipitates with Gal7 and that recombinant Gal7 directly interacts with recombinant Bcl-2. A fraction of Gal7 is constitutively localized at mitochondria in a Bcl-2–dependent manner and sensitizes the mitochondria to the apoptotic signal. In addition, we show that the Bcl-2/Gal7 interaction is abolished following genotoxic stress. Taken together, our findings suggest that the binding of Gal7 to Bcl-2 may constitute a new target for enhancing the intrinsic apoptosis pathway.**

Monitoring Editor
Thomas D. Fox
Cornell University

Received: Jun 23, 2010
Revised: Dec 21, 2010
Accepted: Jan 1, 2011

INTRODUCTION

Metazoa eliminate damaged or infected cells by apoptosis, a program of cell death that is essential for embryogenesis, tissue homeostasis, and defense against pathogens. Defects in apoptosis regulation can lead to cancer, as well as to autoimmune and degenerative diseases (Cory and Adams, 2002). The first apoptotic regulator to be identified through genetic analysis was Bcl-2, an oncoprotein activated via the t(14;18) chromosomal breakpoint in human follicular B-cell lymphoma (Tsujimoto and Croce, 1986). The anti-apoptotic Bcl-2 protein is found in intracellular membranes, such as nuclear envelope, mitochondrial, and endoplasmic reticulum (ER) membranes and is the prototypic member of a large family of apoptosis-regulating proteins that either inhibit or promote cell death (Lithgow *et al.*, 1994). In response to stress stimuli, whether a cell survives or undergoes apoptosis is dependent on the ratio of the pro-apoptotic Bcl-2 family molecules relative to the anti-apoptotic Bcl-2 family members. An imbalance in favor of pro-apoptotic proteins will lead to outer mitochondrial membrane permeabilization, cytochrome *c* release and caspase activation, resulting in the morphological and biochemical changes associated with apoptosis (Brunelle and Letai, 2009). Bcl-2 interacts with a variety of apoptosis-regulating proteins that are members of the Bcl-2 family, such as Bax (Mahajan *et al.*, 1998), Bad (Yang *et al.*, 1995), Bid (Luo *et al.*, 1998), and PUMA (Yu *et al.*, 2001), or are not members of the Bcl-2 family, such as p53 (Chipuk *et al.*, 2004), VDAC (Shimizu *et al.*, 1999), *k*-Ras

This article was published online ahead of print in MBoC in Press (http://www.molbiolcell.org/cgi/doi/10.1091/mbc.E10-06-0534) on February 2, 2011.

Address correspondence to: Florence Larminat (larminat@ipbs.fr).

Abbreviations used: BCAP31, B-cell receptor–associated protein 31; BSA, bovine serum albumin; CRD, carbohydrate recognition domain; DAVID, Database for Annotation, Visualization and Integrated Discovery; EGTA, ethylene glycol tetraacetic acid; ER, endoplasmic reticulum; FDR, false discovery rate; Gal3, galectin-3; Gal7, galectin-7; GST, glutathione *S*-transferase; HM, heavy membrane fraction, IB, immunoprecipitation buffer; ID, internal diameter; IM, mitochondria isolates; IP, immunoprecipitation; LND, lonidamine; MS, mass spectrometry; MS/MS, tandem mass spectrometry; PBS, phosphate-buffered saline; Scr, scrambled siRNA; STRING, Search Tool for the Retrieval of Interacting Genes/Proteins.

(Rebollo *et al.*, 1999), paxillin (Sheibani *et al.*, 2008), and calcineurin (Erin *et al.*, 2003). These data suggest that diverse signaling, developmental, and metabolic pathways converge on Bcl-2. Most of these binding partners have been located at the mitochondria. Deciphering the complete network of Bcl-2 mitochondrial interacting factors should then provide a critical advance in our understanding of the key anti-apoptotic function of Bcl-2.

Here we conducted a global proteomic analysis of Bcl-2 protein immunocomplexes by combining an immunocapture approach using highly purified human mitochondrial fractions with a mass spectrometry (MS) analysis (LTQ Orbitrap). We identified 127 potential direct or indirect Bcl-2–associated partners at high confidence in the immunocomplex. Gene ontology mining revealed enrichment for mitochondrial proteins, ER-associated proteins, and cytoskeleton-associated proteins. Within the complex, we confirmed previously described Bcl-2 binding proteins. Importantly, we report for the first time that galectin-7 (Gal7) is a Bcl-2 interacting protein. Gal7 is a member of a family of soluble β-galactoside–binding lectins that have been shown to have diverse biological functions, including regulation of cell growth, cell adhesion, and apoptosis (Yang and Liu, 2003; Nakahara and Raz, 2006). To date, Gal7, designated as the product of the p53-induced gene 1 (Polyak *et al.*, 1997), is thought to function in stratified epithelial tissue response to environmental injuries, such as wound healing or UV light (Cao *et al.*, 2002; Gendronneau *et al.*, 2008). Gal7 mRNA and protein have been shown to be rapidly induced in skin keratinocytes exposed to UV light and to take part in UV-induced apoptosis (Bernerd *et al.*, 1999; Gendronneau *et al.*, 2008). Interestingly, its overexpression results in cell sensitization to apoptosis triggered by various agents, a process that is caspase-dependent and associated with cytochrome *c* release, strongly suggesting that Gal7 is a pro-apoptotic protein (Kuwabara *et al.*, 2002). It has been postulated that the role of Gal7 on apoptosis is not exerted through the extracellular localization of the lectin, but rather due to its intracellular localization in the nucleus and cytoplasm (Kuwabara *et al.*, 2002).

In the present study, we show that endogenous Gal7 coimmunoprecipitates with endogenous Bcl-2 and that glutathione *S*-transferase (GST)-tagged Gal7 directly interacts in vitro with recombinant Bcl-2. Using fluorescence microscopy, we have established that a fraction of Gal7 is constitutively localized to mitochondria. Furthermore, we found that Gal7 mitochondrial localization is partially dependent on Bcl-2 expression and that overexpression of mitochondrial Gal7 significantly increases cytochrome *c* and Smac/DIABLO release from isolated mitochondria following apoptotic stimulus. Importantly, apoptotic stress triggers increased Gal7 recruitment to mitochondria but disruption of the Bcl-2/Gal7 interaction. Our data establish a novel pathway linking pro-apoptotic Gal7 and anti-apoptotic Bcl-2 and, ultimately, apoptosis.

RESULTS

Bcl-2–associated proteins identified by LTQ Orbitrap analysis

To identify new endogenous mitochondrial Bcl-2–associated proteins, we used an immunoaffinity capture technique applied to HCT16 colon carcinoma cells' highly purified mitochondria followed by mass spectrometry–based identification of copurifying Bcl-2 partners. Mitochondria isolates (IM) obtained by differential centrifugations and sucrose gradient were free of nuclear contamination as compared with crude mitochondria (heavy membrane fractions [HMs]) obtained by differential centrifugations only, as confirmed by the absence of the PCNA marker on immunoblot analysis for the status of mitochondrial subcellular fractions isolated from HCT116

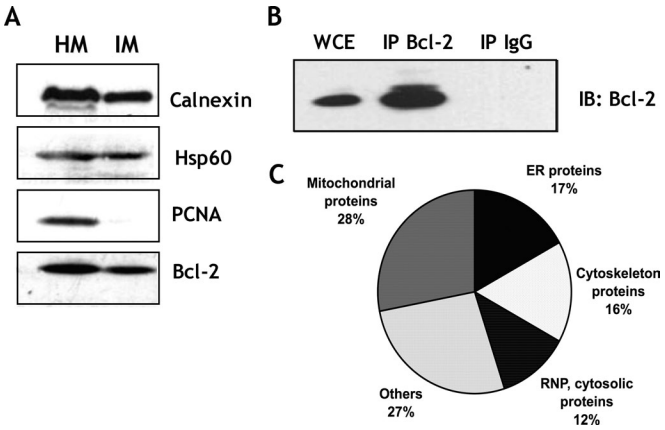

FIGURE 1: Analysis of Bcl-2 immunocomplexes isolated from mitochondrial fractions. (A) Purity of mitochondrial fraction (IM) isolated from HCT116 cells and used for MS was assessed by detection of nuclear factor PCNA, ER protein calnexin, and mitochondrial protein Hsp60 by immunoblot. (B) Bcl-2 is specifically immunoprecipitated from mitochondrial extracts. Bcl-2 IP was performed with a pool of monoclonal and polyclonal anti-Bcl-2 antibodies and negative control IP using isotype-matched nonrelevant antibodies. Both IPs were performed with 500 µg of lysed mitochondria incubated with protein A–coated sepharose beads. The presence of Bcl-2 was analyzed by immunoblotting (n = 3). (C) Distribution of enriched classes of Bcl-2–associated proteins identified by the LTQ-Orbitrap analysis was obtained using the DAVID database bioinformatics resource. The threshold for statistical significance is <0.001.

cells (Figure 1A). IMs still contain some ER-associated proteins, such as calnexin (Figure 1A). Mitochondrial proteins were then solubilized with CHAPS, a detergent that does not alter authentic binding interactions of Bcl-2 family proteins (Antonsson, 2001). Bcl-2 immunoprecipitation (IP) was performed with a pool of monoclonal and polyclonal anti-Bcl-2 antibodies and negative control IP (IP IgG) using isotype-matched irrelevant antibodies (Figure 1B). Following protein separation by one-dimensional SDS–PAGE and visualization by Coomassie Brilliant Blue staining, 20 equal gel slices (regardless of staining) were excised from both lanes, processed for in-gel tryptic digestion of proteins, and subjected to mass spectrometry–based proteomics. Mascot results files were parsed automatically, and protein hits were validated using different criteria based on the number, rank, and score of the assigned peptides (as described in *Materials and Methods*). Multiple peptides corresponding to the same protein strengthened the identification. Proteins identified with a single peptide were confirmed by manual inspection of the tandem mass spectrometry (MS/MS) spectra. The results were considered to be relevant if the false-positive rate never exceeded 1%. For reproducibility, Bcl-2 and control IP experiments were performed in duplicate.

To select for proteins that interact specifically with Bcl-2 and not those that associate with IgG or beads in an unspecific manner, we subtracted proteins that were common between Bcl-2 and control IP lanes. After subtracting unspecific proteins, a total of 127 unique proteins that potentially interact with Bcl-2 were identified from two independent experiments and pooled in Table 1. Importantly, Bcl-2 was successfully immunopurified and identified by MS when anti-Bcl-2 antibodies were used (Table 1). Among listed Bcl-2 partners, PUMA (Bcl-2 binding component 3) (Yu *et al.*, 2001), BNIP1 (also known as NIP1, SEC20, or TRG-8) (Boyd *et al.*, 1994), and BCAP31 (B-cell receptor–associated protein 31) (Ng *et al.*, 1997), well-known

Accession number	Description	Matched peptides	Coverage (%)
	Mitochondrial proteins		
A8K5F1	Highly similar to human DEAH – Human	1	0.7
Q9NRK6	ATP-binding cassette, mitochondrial precursor – Human	2	2.7
P28838	Cytosol aminopeptidase – Human	1	2.3
P27338	Amine oxidase (flavin-containing) B – Human	2	3.3
Q9BXH1	Bcl-2-binding component 3 PUMA – Human	1	7
P10415	Apoptosis regulator Bcl-2 – Human	4	22
P04040	Catalase – Human	3	7
P10606	Cytochrome *c* oxidase subunit, mitochondrial precursor – Human	5	30.2
Q8N2U0	UPF0451 protein C17orf61 precursor – Human	1	24.8
Q9NVH1	DnaJ homologue subfamily C member 11 – Human	7	10.4
Q96LJ7	Dehydrogenase/reductase SDR family member 1 – Human	4	12.1
P43003	Excitatory amino acid transporter 1 – Human	1	2.2
O43837	Isocitrate dehydrogenase subunit, mitochondrial precursor – Human	4	9.4
Q5VT66	MOSC domain-containing protein 1, mitochondrial precursor – Human	3	9.8
O75431	Metaxin-2 – Human	2	7.2
O75438	NADH dehydrogenase [ubiquinone] 1 beta subcomplex subunit 1 – Human	2	32.8
P19404	NADH dehydrogenase flavoprotein 2, mitochondrial precursor – Human	4	16.5
P08559	Pyruvate dehydrogenase E1 component α subunit, mitochondrial protein – Human	6	13
Q15070	Inner membrane protein OXA1L, mitochondrial precursor – Human	1	2.3
O60437	Periplakin (195 kDa cornified envelope precursor protein) – Human	2	1
P30048	Thioredoxin-dependent peroxide reductase, mitochondrial precursor – Human	2	9
Q02127	Dihydroorotate dehydrogenase, mitochondrial precursor – Human	3	10.6
Q3B7×4	IMMT protein – Human	19	41.1
Q561V6	NDUFB5 protein – Human	2	13.9
Q5W145	NADH dehydrogenase – Human	4	29
Q6ICN9	NDUFB7 protein – Human	3	25.5
Q6P1S1	Mitochondrial ribosomal protein S27 – Human	2	5
Q85KX8	Cytochrome *c* oxidase subunit 2 – Human	10	35.2
Q7L0Y3	RNA methyltransferase domain–containing protein 1 – Human	4	8.6
Q6FG42	NDUFA7 protein – Human	3	22
Q9UHQ9	NADH-cytochrome b5 reductase 1 – Human	1	3.6
P09211	GST P – Human	1	5.2
Q9H3K2	Growth hormone–inducible transmembrane protein – Human	1	3.2
Q15070	Inner membrane protein OXA1L, mitochondrial precursor – Human	1	2.3
Q9NVA1	Ubiquinol-cytochrome *c* reductase complex CBP3 homologue – Human	1	3

Bcl-2 was immunoprecipitated with a pool of anti-Bcl-2 antibodies from 1 mg of highly purified mitochondrial extracts isolated from human HCT116 cells. Negative control IP was performed using isotype-matched nonrelevant antibodies. Immunocaptured proteins from both IPs were subjected to MS analysis. Proteins that are common between Bcl-2 and control IP are subtracted to select for a set of proteins that specifically interact with Bcl-2. A total of 127 unique proteins were identified from two independent experiments, pooled, and classified according to their cellular localization using the DAVID database bioinformatics resource.

TABLE 1: Protein identification in Bcl-2 immunocomplexes by LTQ-Orbitrap analysis.

(Continues)

Accession number	Description	Matched peptides	Coverage (%)
	ER-associated proteins		
A4D1F8	Cytochrome P450, family 51, subfamily A, polypeptide 1 – Human	1	2.8
A8K1G0	Highly similar to SEC22 vesicle trafficking protein-like 1 – Human	8	37.7
P02647	Apolipoprotein A-I precursor (Apo-AI) – Human	1	6
P51572	BCAP31 – Human	6	21.5
P10415	Apoptosis regulator Bcl-2 – Human	4	22
Q9UBM7	7-dehydrocholesterol reductase – Human	7	13.5
Q9P2x0	Dolichol-phosphate mannosyltransferase subunit 3 – Human	1	10.9
Q14165	Uncharacterized protein KIAA0152 precursor – Human	5	16.8
Q96G23	LAG1 longevity assurance homologue 2 – Human	1	4.2
Q12907	Vesicular integral-membrane protein VIP36 precursor – Human	6	15.4
Q86UE4	Protein LYRIC – Human	2	3.8
P30101	Protein disulfide-isomerase A3 precursor – Human	2	4
Q5VWA5	Dolichyl-diphospho-oligosaccharide-protein glycosyltransferase – Human	9	22.6
Q7LA14	KIAA0851 protein – Human	3	5
Q9HBH5	Retinol dehydrogenase 14 – Human	1	3.9
Q6NUM9	All-transretinol 13,14-reductase precursor – Human	2	3.9
O00560	Syntenin-1 – Human	2	9.7
Q12981	Vesicle transport protein SEC20, BNIP1 – Human	1	3.9
P08240	Signal recognition particle receptor subunit alpha – Human	7	8.9
P46977	Dolichyl-diphosphoo-ligosaccharide-glycosyltransferase subunit STT3A – Human	8	10.5
Q9BVC6	Transmembrane protein 109 precursor – Human	3	9.1
Q9BVK6	Transmembrane emp24 domain–containing protein 9 precursor – Human	6	19.2
Q8WY22	BRI3-binding protein – Human	4	19.5
	Cytoskeleton associated proteins		
O14639	Actin-binding LIM protein 1 – Human	2	2.3
P12814	Alpha-actinin-1 (Alpha-actinin cytoskeletal isoform) – Human	3	4
P04083	Annexin A1 (Annexin I) (Lipocortin I) (Calpactin II) – Human	1	3
P61160	Actin-related protein 2 – Human	8	16.5
O15144	Actin-related protein 2/3 complex subunit 2 – Human	6	18.3
P07384	Calpain-1 catalytic subunit – Human	1	1.4
P47755	F-actin-capping protein subunit alpha-2 – Human	9	22.7
Q16643	Drebrin – Human	15	26.5
O75955	Flotillin-1 – Human	1	3.3
P07476	Involucrin – Human	4	7
P24844	Myosin regulatory light chain 2, smooth muscle isoform – Human	8	44.2
Q96SB3	Neurabin-2 – Human	4	4.3
Q13835	Plakophilin-1 – Human	4	6
Q8WVV4	Protein POF1B (Premature ovarian failure protein 1B) – Human	3	6
P07737	Profilin-1 (Profilin I) – Human	2	19
Q53HG7	Cortactin isoform a variant – Human	6	11.5
Q9NSU9	Hypothetical protein DKFZp434G0719 (Fragment) – Human	3	9
Q13813	Spectrin alpha chain, brain – Human	5	1.9
Q9NYL9	Tropomodulin-3 – Human	11	30.4
Q13049	Tripartite motif–containing protein 32 – Human	7	11

TABLE 1: Protein identification in Bcl-2 immunocomplexes by LTQ-Orbitrap analysis. (Continued)

Accession number	Description	Matched peptides	Coverage (%)
	Ribonucleoproteins, cytosolic proteins		
Q10567	AP-1 complex subunit beta-1 – Human	3	3.5
O75531	Barrier-to-autointegration factor – Human	1	27
P09104	Gamma-enolase (2-phospho-D-glycerate hydro-lyase) – Human	2	6
Q14677	Clathrin interactor 1 – Human	4	7.8
P38159	Heterogeneous nuclear ribonucleoprotein G – Human	5	12
Q14974	Importin subunit beta-1 – Human	1	1.7
Q53F64	Heterogeneous nuclear ribonucleoprotein AB isoform a variant – Human	1	4.2
Q5JR94	Ribosomal protein S8 – Human	3	15.9
P39023	60S ribosomal protein L3 – Human	2	4.2
Q9Y3U8	60S ribosomal protein L36 – Human	2	19
P15880	40S ribosomal protein S2 – Human	2	8.2
P08865	40S ribosomal protein SA – Human	2	7.8
O95816	BAG family molecular chaperone regulator 2 – Human	3	14.2
Q8IZD9	Dedicator of cytokinesis protein 3 – Human	1	0
Q5TBM7	Heat shock 105 kDa protein 1 – Human	1	1
O75330	Hyaluronan mediated motility receptor – Human	10	13
	Others		
A0FGR9	Extended-synaptotagmin 3 – Human	2	1
A2RUI1	Desmoglein 4 – Human	2	2
A5PLL2	FUT8 protein – Human	1	4.5
A6NN19	Uncharacterized protein ENSP00000309842 – Human	3	9
A8K287	Highly similar to synaptosomal-associated protein – Human	2	10
A8K3P8	Highly similar to Human TPA regulated locus – Human	1	3.4
A8K6H9	Highly similar to solute carrier family 38, member 2 – Human	2	5.3
P28288	ATP-binding cassette subfamily D member 3 – Human	4	5.6
O94766	Galactosylgalactosylxylosylprotein 3-beta-glucuronosyltransferase 3 – Human	1	2.7
P27482	Calmodulin-like protein 3 – Human	4	24.2
O60911	Cathepsin L2 precursor – Human	1	4.2
O00257	E3 SUMO-protein ligase CBX4 – Human	2	2.3
Q494V2	Coiled-coil domain–containing protein 37 – Human	1	1
Q16610	Extracellular matrix protein 1 precursor – Human	1	2.4
P02765	Alpha-2-HS-glycoprotein precursor (Fetuin-A) – Human	4	7
Q14254	Flotillin-2 – Human	3	7.1
P42167	Lamina-associated polypeptide 2, isoforms beta/gamma – Human	3	3.7
Q86×29	Lipolysis-stimulated lipoprotein receptor – Human	10	17.3
O15427	Monocarboxylate transporter 4 – Human	4	9.5
Q4LE60	TNPO2 variant protein (Fragment) – Human	1	1
Q5K680	F-box only protein 31 – Human	1	1
Q5RHS6	S100 calcium binding protein A16 – Human	1	11
Q5TG62	KIAA0090 – Human	4	4.1
Q6E0U4	Dermokine-beta (Dermokine) – Human	2	4
Q6IB87	LGALS7 protein – Human	16	77
Q6U2F4	C4A – Human	2	1.5
Q6UWP8	HLAR698 (Suprabasin) – Human	3	13

TABLE 1: Protein identification in Bcl-2 immunocomplexes by LTQ-Orbitrap analysis. (Continued)

Accession number	Description	Matched peptides	Coverage (%)	Accession number	Description	Matched peptides	Coverage (%)
Q6ZSA9	CDNA FLJ45682 fis, clone FCBBF3001018 – Human	1	2	P23246	Splicing factor, proline- and glutamine-rich – Human	2	3
Q96JG3	KIAA1864 protein (Fragment) – Human	3	3	P36952	Serpin B5 precursor (Maspin) (Protease inhibitor 5) – Human	1	3
Q6NTF9	Rhomboid domain-containing protein 2 – Human	1	4.4	P05543	Thyroxine-binding globulin precursor (Serpin A7) – Human	1	2
P31949	Protein S100-A11 (S100 calcium-binding protein A11) – Human	1	15	P02788	Lactotransferrin precursor – Human	2	2.7

TABLE 1: Protein identification in Bcl-2 immunocomplexes by LTQ-Orbitrap analysis. (Continued)

Bcl-2 interacting proteins, were clearly identified and validated the co-IP experiment and the MS data (Table 1). Bcl-2–associated proteins were automatically sorted according to their cellular and functional distribution using the Database for Annotation, Visualization and Integrated Discovery (DAVID) Gene Functional Classification Tool (http://david.abcc.ncifcrf.gov) and list of UniProt identifiers. Statistically significant ($p < 0.001$) biological process terms from the Gene Ontology project were determined among the set of proteins. The major class corresponds to components of the mitochondria (28%) and is linked to known mitochondrial pathways, in accordance with the location of Bcl-2 at the mitochondrial membrane (Figure 1C). Other classes mainly represented include the ER (17%), the cytoskeleton (16%), and, to a lesser extent, ribonucleoproteins and cytosolic proteins (12%) (Figure 1C).

Gal7 is a novel Bcl-2–binding protein

To further examine the proteins interacting with Bcl-2, we used the Search Tool for the Retrieval of Interacting Genes/Proteins (STRING) database to extract enriched functional protein clusters (http://string.embl.de/version_6_2). Previously established criteria were applied to identify reliable physical protein–protein interactions. Hierarchical clustering provided a statistical approach to identifying distinct protein complexes from a large number of proteins that were immunoaffinity purified and analyzed by MS. Reported interactions may correspond to proteins that interact directly or, probably more frequently, correspond to proteins that interact indirectly, via one or more bridging molecules. As shown in Figure 2, the protein network includes three major distinct functional clusters: a mitochondrial cluster containing subunits of the NADH dehydrogenase complex (NDU proteins; Figure 2A), a cluster containing ribosomal proteins (RNP proteins; Figure 2B), and a cluster containing the Bcl-2 protein and its known partners (Figure 2C).

Interestingly, Gal7 (ENSG000001178934; Figure 2D), known to exhibit a pro-apoptotic function, was not assigned to any functional class and was detected as a novel Bcl-2 interacting protein in two independent Bcl-2 IP experiments performed with HCT116 mitochondrial extracts (Table 1). The covering sequence reached 77%, and 16 peptides were detected, allowing unambiguous identification of the protein (Table 2 and Figure 3). We confirmed the endogenous Bcl-2/Gal7 interaction highlighted in Bcl-2 IP MS data by performing reciprocal IP using HCT116 mitochondrial extracts and anti-Gal7 serum (Figure 4A). To further validate this interaction, we

m/z	Charge	Experimental mass	Theoretical mass	Mass difference	Sequence	Position in the protein sequence
429.23	2	856.45	856.46	−0.001	GPGVPFQR	76–83
431.77	2	861.53	861.53	−0.0004	HRLPLAR	112–118
455.76	2	909.5	909.5	−0.0007	GLVPPNASR	24–32
590.35	2	1178.69	1178.69	−0.0015	IRGLVPPNASR	22–32
411.85	3	1232.55	1232.55	0.0009	EQGSWGREER	66–75
619.82	2	1237.62	1237.62	−0.0015	LDTSEVVFNSK	55–65
636.33	2	1270.64	1270.64	−0.0017	EERGPGVPFQR	73–83
700.35	2	1398.68	1398.68	−0.0022	AVVGDAQYHHFR	100–111
494.62	3	1480.83	1480.84	−0.0012	SSLPEGIRPGTVLR	8–21
743.4	2	1484.78	1484.78	−0.0009	LVEVGGDVQLDSVR	121–134
868.45	2	1734.88	1734.88	0.0001	GQPFEVLIIASDDGFK	84–99
580.99	3	1739.95	1739.95	−0.0026	VRLVEVGGDVQLDSVR	119–134

Peptide masses determined by LTQ-Orbitrap analysis of the tryptic digest of Gal7 are compared with the theoretical mass resulting from the Swiss-Prot database search. Corresponding mass differences, peptides sequences, and position in the protein sequence are indicated. The matched peptides cover 77% of the protein sequence.

TABLE 2: Identification of Gal7 by LTQ Orbitrap mass fingerprint and database search.

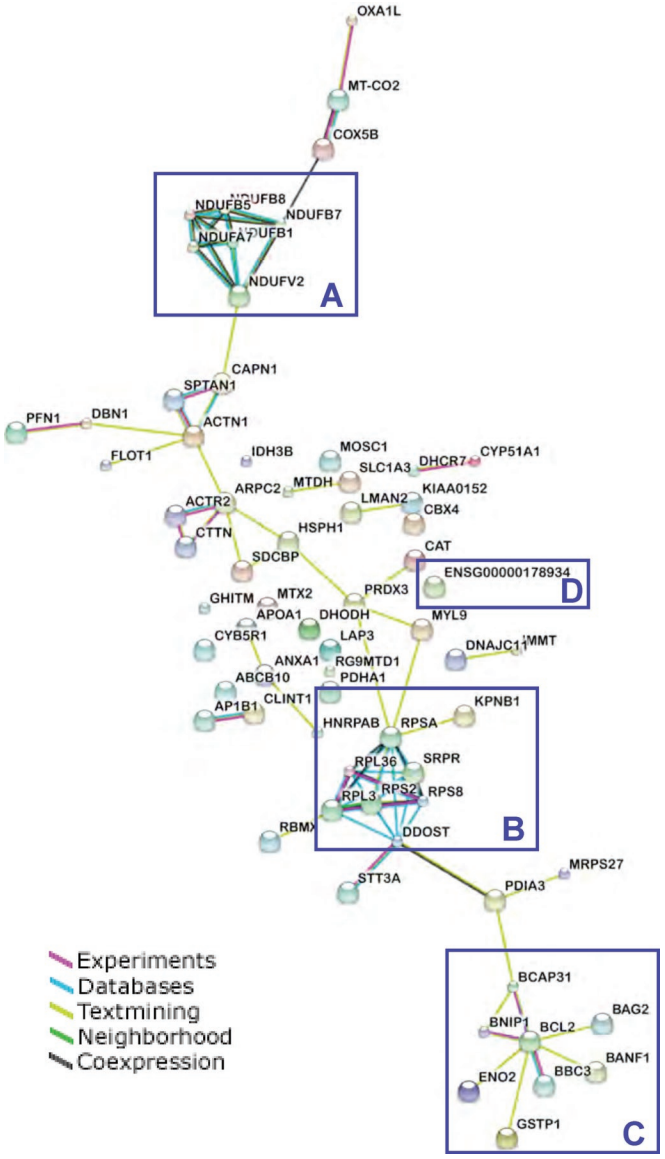

FIGURE 2: Pathway network from STRING showing a set of proteins associated with Bcl-2 in HCT116 cells. Protein–protein interaction map of Bcl-2–associated proteins was obtained using STRING database. Network map was created with default settings, allowing for experimentally verified and predicted interactions. In the network, links between proteins signify the various interaction data supporting the network, colored by evidence type. (A) NDU cluster (NADH dehydrogenase complex); (B) RNP cluster (ribosomal proteins); (C) Bcl-2 cluster; (D) Gal7.

used Gal7-overexpressing HeLa cells (HeLa-G7) together with their control HeLa-v cells that were obtained from Fu-Tong Liu (Kuwabara *et al.*, 2002). As shown in Figure 4B, Gal7 was also coimmunoprecipitated following Bcl-2 IP performed with mitochondrial extracts isolated from Gal7-overexpressing HeLa cells. In contrast, Hela-v cells transfected with the empty pEF1-neo vector scarcely express Gal7 and did not allow the observation of Gal7/Bcl-2 association (Figure 4B). These data, along with the MS results, clearly demonstrate that Gal7 is a novel Bcl-2 interacting protein.

Bcl-2 directly associates with Gal7 in vitro independently of Gal7 carbohydrate recognition domain

Because data obtained from co-IP experiments did not discriminate between direct and indirect types of interaction, we further investigated the interaction of Gal7 with Bcl-2 using recombinant purified proteins. We produced an N-terminal GST-Gal7 protein that was expressed and purified as previously described (Magnaldo *et al.*, 1995) and used a recombinant purified Bcl-2 protein without its C-terminal transmembrane domain. GST pull-down results confirmed co-IP findings in that Bcl-2 associated with Gal7 and further demonstrated that there is a direct interaction between the two proteins (Figure 5, A and B). We observed only weak binding of Bcl-2 using GST-alone pull-down, indicating the specificity of our binding results (Figure 5A).

All galectins share affinity for β-galactoside, such as lactose, thanks to their carbohydrate recognition dDomain (CRD). Some intracellular galectin-binding proteins have been recently identified (Rapoport *et al.*, 2008). Although not glycosylated, these proteins interact with galectins through their CRD. Therefore we investigated whether Gal7 interaction with Bcl-2 could involve its CRD using an in vitro GST-pulldown competition assay. Increasing concentrations up to 100 mM lactose had no effect on recombinant Bcl-2 binding to GST-Gal7 fusion protein, indicating that Bcl-2 and Gal7 interaction does not involve Gal7 CRD (Figure 5, A and B).

Gal7 is constitutively localized to mitochondria

Our results showing a striking association of Gal7 with Bcl-2 using highly purified mitochondrial cell extracts predicted the presence of Gal7 at the mitochondrial membrane. Previous studies have shown that Gal7 is found in the cytoplasm, in the nucleus, and in the extracellular space (Kuwabara *et al.*, 2002), but, so far, it has never been localized to mitochondria. To demonstrate that endogenous Gal7 is also localized to mitochondria, we performed immunoblot analysis using mitochondria-enriched fractions recovered from HaCaT, HCT116, and HeLa cell lines. The transformed keratinocyte HaCaT cell line is known to express Gal7 at a significant level (Kuwabara *et al.*, 2002), whereas HeLa cells scarcely express it. As shown in Figure 6A, Gal7 was strongly detected in mitochondrial fractions obtained from both HaCaT and HCT116 cells but only weakly present in HeLa mitochondrial extracts. The size of the mitochondrial Gal7 protein detected in the three cell lines was similar to the apparent molecular size of the recombinant Gal7 that was loaded onto the gel as standard (Figure 6A).

To further confirm the mitochondrial Gal7 localization, we examined its subcellular localization by indirect immunofluorescence staining and microscope analysis. As indicated by overlapping of immunostainings obtained in a series of denoised focal planes, Gal7 and the mitochondrial marker Hsp60 partially colocalized in HCT116 cells (Figure 6B). Similar colocalization was observed in HaCaT and HeLa cells (unpublished data). We confirmed the specificity of the anti-Gal7 antibody by performing a blocking experiment using the immunogen (Magnaldo *et al.*, 1998) (Figure 6C). In support of this result, anti-Gal7 antibody immunoreactivity was not detected in Gal7-null mice epidermis (Gendronneau *et al.*, 2008). Altogether our data demonstrate that a portion of Gal7 is constitutively localized to mitochondria in addition to its already known locations.

Bcl-2 contributes to Gal7 targeting to mitochondria

Although Gal7 is localized to mitochondria, it obviously lacks signal sequences for its mitochondrial targeting. These data suggest that Gal7 recruitment to mitochondria may occur through its interaction with other proteins. To determine whether Bcl-2 may contribute to Gal7 mitochondrial targeting, we silenced Bcl-2 expression using siRNA in HeLa-Gal7 cells, in which Gal7 was shown to be located at mitochondria (Figure 4B). As indicated in Figure 6D, 48 h after transfection, total Bcl-2 expression was almost completely inhibited by Bcl-2–targeted siRNA but not by unspecific scramble siRNA. Importantly, our results show that siRNA silencing

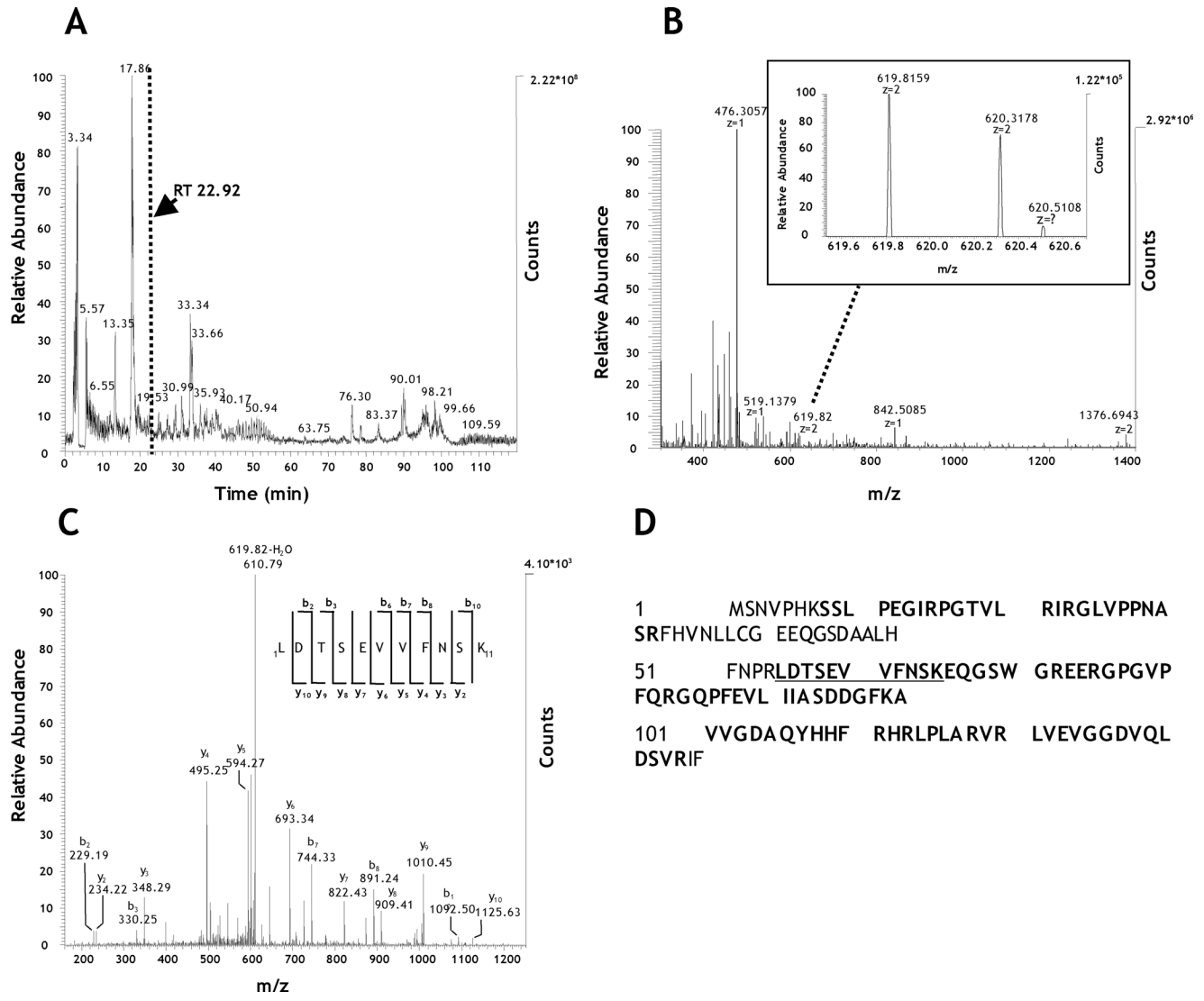

FIGURE 3: Identification of Gal7 as a novel Bcl-2–interacting protein by LTQ-Orbitrap MS. Bcl-2 was immunoprecipitated from highly purified mitochondria isolated from HCT116 cells. Proteins were resolved by SDS–PAGE, and their tryptic digests were analyzed by LTQ-Orbitrap MS. (A) Total ion chromatogram of the tryptic digest containing Gal7. An arrow at 22.92 min indicates the retention time of one of the peptides that allowed the identification of Gal7. (B) MS spectrum at 22.92-min retention time with an expanded view in a narrow *m/z* range around the doubly charged peptide at *m/z* 6190.8159. (C) MS/MS spectrum of the doubly charged precursor ion at *m/z* 619.82 corresponding to the peptide sequence LDTSEVVFNSK of the Gal7 protein. (D) Sequence coverage. The identified peptide sequences (listed in Table 2) are indicated in bold, and the underlined sequence corresponds to the MS/MS spectrum shown in (C) (n = 2).

of Bcl-2 significantly decreases the amount of Gal7 at the mitochondria, but not at the whole cell level (Figure 6D). Thus our data indicate that Bcl-2 contributes, at least partially, to Gal7 targeting to mitochondria.

Isolated mitochondria overexpressing Gal7 are more sensitive to apoptotic stimulus

Gal7 expression is induced following exposure to UV irradiation, and an increased level of the protein was found in sunburned apoptotic keratinocytes (Bernerd *et al.*, 1999). Moreover, Gal7 overexpression has been shown to increase susceptibility of HeLa cells to apoptosis triggered by several distinct apoptotic stimuli (Kuwabara *et al.*, 2002). With regard to the pro-apoptotic function of Gal7, we then investigated the effects of Gal7 overexpression on apoptosis sensitivity induced by UV exposure. HeLa-G7 and HeLa-v cells were UV-irradiated at 60 J/m^2 and then harvested at various time points for immunoblotting analysis. Apoptosis sensitivity was assessed in whole-cell extracts by detection of early biochemical events in this process. As shown in Figure 7A, both poly (ADP-ribose) polymerase (PARP) proteolysis and caspase-3 activation were substantially accelerated in HeLa-G7 over HeLa-v cells after UV. These data indicate that Gal7 overexpression results in enhanced sensitivity to apoptosis induction upon UV exposure and are consistent with those reported by Kuwabara *et al.* (2002) showing increased amounts of annexin V–positive cells among UV-irradiated HeLa-G7 cells compared with parental cells.

Because our present data demonstrate the presence of Gal7 at mitochondria (Figures 4 and 6), we next examined the importance of mitochondrial targeting of Gal7 in its pro-apoptotic function. To address this issue, we investigated whether increased amounts of

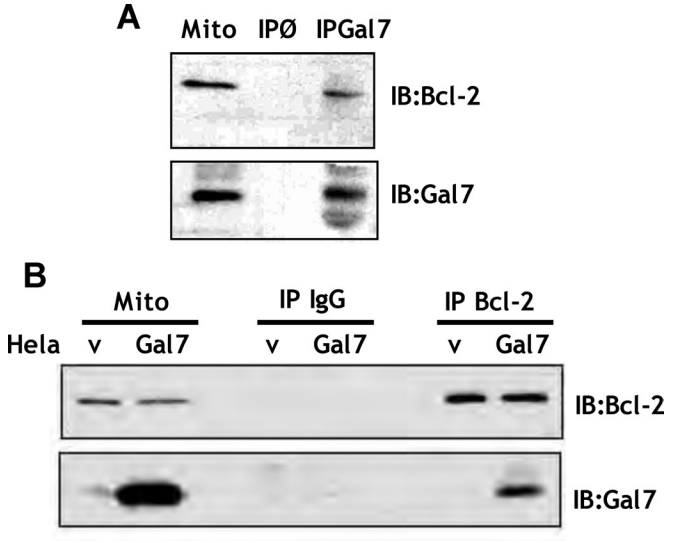

FIGURE 4: Gal7 association with Bcl-2 in mitochondria. (A) Mitochondria were purified from HCT116 cells by differential centrifugation, and Gal7 was immunoprecipitated using protein A–coated sepharose beads and anti-Gal7 serum. The presence of Gal7 and Bcl-2 in whole mitochondrial extracts (M) and in mitochondrial immunoprecipitates (IP) was analyzed by immunoblotting. IPϕ, control IP with sepharose beads alone (n = 4). (B) Mitochondria were obtained by differential centrifugation from HeLa cells stably transfected with Gal7 containing vector (HeLa-Gal7) or empty vector (HeLa-v). For IP, 500 µg of lysed mitochondria were incubated with protein A–coated sepharose beads in the presence of anti-Bcl-2 antibodies (IP Bcl-2) or with nonrelevant antibodies (IP IgG). The precipitated proteins were visualized by immunoblotting (IB). Mito: 50 µg of total lysed mitochondria (n = 2).

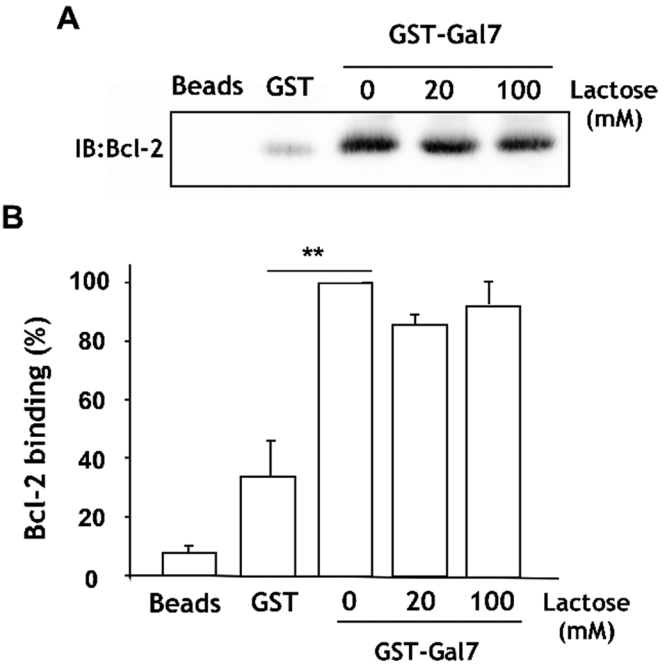

FIGURE 5: Direct Gal7 interaction with Bcl-2 in a lactose-independent way. GST or GST-Gal7 fusion proteins bound to glutathione-sepharose beads were incubated with 0.1 µg of recombinant Bcl-2 in the absence or presence of lactose at the indicated concentrations. Bcl-2 proteins eluted from the beads were detected by immunoblot analysis using anti–Bcl-2 antibody. (A) Representative immunoblot from a GST pull-down experiment. (B) Quantification of six experiments using ImageJ software. Recombinant Bcl-2 binding to GST-Gal7 beads was arbitrarily fixed to 100%. Comparison of mean values between Bcl-2 binding on GST beads and on GST-Gal7 beads was assessed with Student's *t* test: $p < 0.01$.

Gal7 at mitochondria could sensitize purified intact mitochondria to the action of direct pro-apoptotic agents. To mimic apoptotic induction on purified mitochondria, we used lonidamine (LND), an activator of the mitochondrial transition-permeability pore opening and tBid, a BH3-only member of the Bcl-2 family, which are well-known inducers of the release of mitochondrial apoptogenic mediators, such as cytochrome *c* and Smac/DIABLO.

Intact mitochondria isolated from HeLa-G7 overexpressing Gal7 and HeLa-v parental cells were incubated for 20 min with 16 nM tBid or 25 mM LND and analyzed in terms of release of pro-apoptotic factors from the mitochondrial intermembrane space. Smac/DIABLO and cytochrome *c* protein contents released from untreated (Cont) or treated (LND and tBid) mitochondria were analyzed by immunoblotting (Figure 7B, Supernatant). Immunoblot analysis of pellet fractions using anti-Hsp60 antibody confirmed input of equivalent amounts of mitochondria for all samples (Figure 7B, Pellet). Cytochrome *c* and Smac/DIABLO were scarcely released in the supernatant of untreated mitochondria (Figure 7B, lanes Cont). On the contrary, tBid or LND treatments triggered cytochrome *c* and Smac/DIABLO release from mitochondria, as indicative of the apoptotic process (Figure 7B, lanes tBid and LND). Importantly, our data showed that overexpression of Gal7 enhances the ability of LND and tBid to induce cytochrome *c* and Smac/DIABLO release from mitochondria (HeLa-G7) when compared with parental mitochondria (HeLa-v) (Figure 7B). Immunoblot analysis indicates that overexpression of mitochondrial Gal7 results in a twofold increase of cytochrome *c* and Smac/DIABLO release following tBid treatment and a 2.5-fold increase of cytochrome *c* and Smac/DIABLO release following LND treatment (Figure 7B, HeLa-G7 vs. HeLa-v lanes). Taken together, our results clearly indicate that mitochondrial Gal7 overexpression sensitizes the mitochondria to the apoptotic signal. They suggest that mitochondrial Gal7 may directly contribute to apoptosis signaling.

It should be noted that direct incubation of intact mitochondria isolated from HeLa-v cells with recombinant Gal7 protein alone did not induce the release of cytochrome *c* and Smac/DIABLO (unpublished data). This result suggests that Gal7 has a weaker pro-apoptotic activity than BH3-only proteins such as Bid or needs to be activated in response to apoptotic stimuli to contribute to cytochrome *c* release.

Gal7/Bcl-2 interaction is disrupted following UV irradiation

To further address the biological significance of the Bcl-2/Gal7 association, we asked whether Gal7 recruitment to mitochondria could be regulated by an apoptotic signal. We then exposed or not HCT116 cells to UV light at a dose of 40 J/m^2 to observe Gal7 presence at mitochondria at various post-UV time points and performed indirect immunofluorescence staining and microscope analysis. As indicated by overlapping of immunostainings obtained in a series of denoised focal planes, Gal7 is more abundant in mitochondria from UV-irradiated cells (UV) than from untreated cells (NT) (Figure 8A). Maximal mitochondrial Gal7 accumulation was observed 9 h following UV exposure (Figure 8A). It has to be noted that UV-irradiated cell morphology was examined at that post-UV time point without noticing the presence of precocious apoptotic bodies (unpublished data). Moreover, increased recruitment of Gal7 to mitochondria was also observed following other genotoxic stress, such as cisplatin treatment (unpublished data).

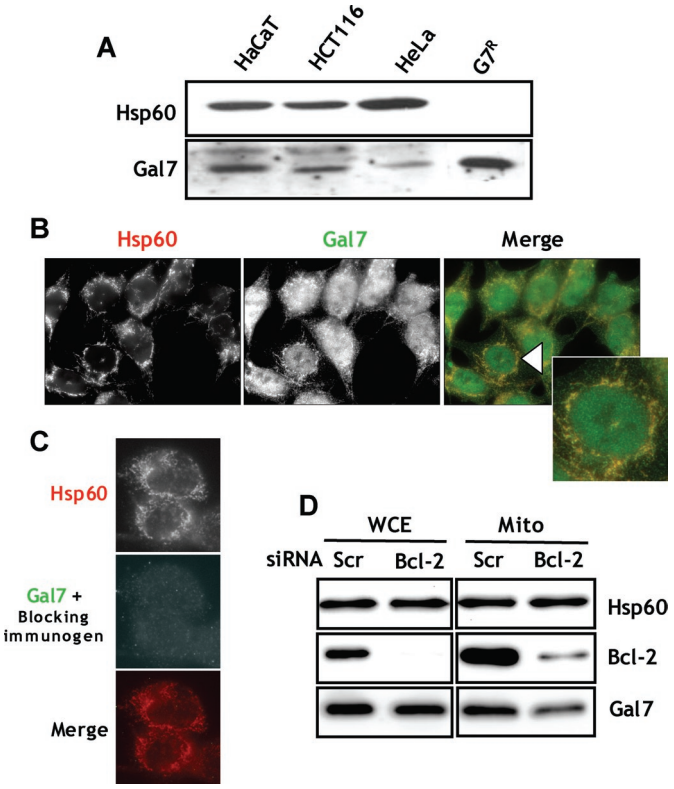

FIGURE 6: Constitutive Gal7 localization to mitochondria. (A) Mitochondria from HCT116, HeLa, or HaCaT cells were isolated by differential centrifugation. Mitochondrial extracted proteins were loaded onto 12% SDS–PAGE and incubated with antibodies raised against Gal7 or the mitochondrial matrix protein Hsp60. Recombinant Gal7 ($G7^R$) was used as migration standard and Hsp60 for mitochondrial marker and loading control (n = 3). (B) HCT116 cells were coimmunostained with anti-Gal7 antibody and anti-Hsp60 antibody. Hsp60 and Gal7 stainings are presented as monochrome images. For overlay, Hsp60 was assigned a red staining and Gal7 a green one. Bar = 5 mm. n = 4. (C) Nonspecific binding of polyclonal Gal7 antibody was determined after binding of the antibody to its blocking immunogen for 2 h. Hsp60 and Gal7 stainings are presented as monochrome images. For overlay, Hsp60 was assigned a red staining and Gal7 a green one (n = 2). (D) HeLa-Gal7 cells were transfected with Bcl-2 siRNA or control Scr duplexes. 48 h after transfection, whole-cell extracts (WCE) and mitochondrial extracts (Mito) were obtained from transfected cells to assess Bcl-2 and Gal7 protein amounts by immunoblot (n = 3).

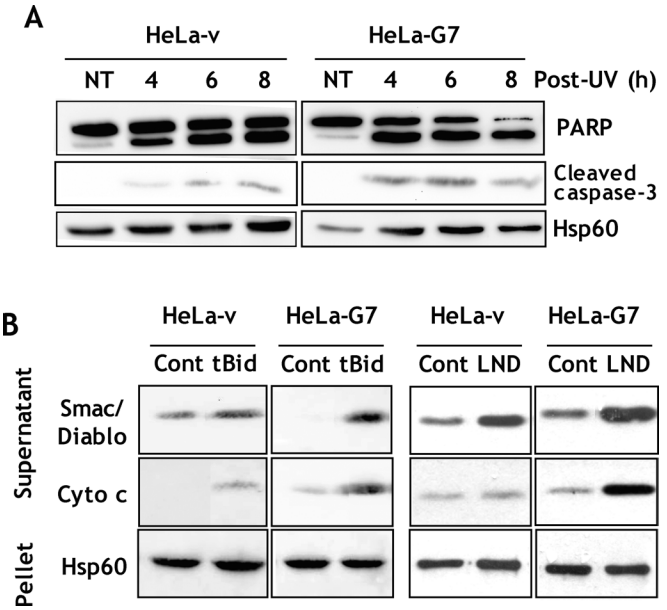

FIGURE 7: Enhanced mitochondria sensitization to apoptotic stimulus by Gal7 overexpression. (A) HeLa-G7 and parental HeLa-v cells were harvested at various time points following UV irradiation at 60 J/m^2 or left untreated (NT). Apoptosis induction was assessed in total cell extracts by detection of PARP cleavage and caspase-3 activation by immunoblotting (n = 2). (B) Intact mitochondria were isolated from HeLa-G7 cells and parental HeLa-v cells and then incubated for 20 min in vitro with 16 nM tBid or 25 μM LND. Following centrifugation, proteins contained in supernatants were resolved to SDS–PAGE and immunoblotted with anti–cytochrome c and anti-Smac/DIABLO antibodies. Cont: untreated mitochondria. Immunoblot analysis of pellet fractions using anti-Hsp60 antibody confirmed input of equivalent amounts of mitochondria for all samples (n = 3).

To confirm mitochondrial Gal7 accumulation, we isolated highly purified mitochondria for 9 h following UV irradiation from UV-treated and untreated cells. The Gal7 amounts were then analyzed by immunoblotting at the whole-cell level (WCE) and at the mitochondrial level (Mito) (Figure 8B). Our results indicate that Gal7 is substantially recruited to mitochondria 9 h following UV exposure when its total amount is only slightly increased at the whole-cell level (Figure 8B). Because the mitochondrial fraction that we used was contaminated with ER (Figure 1A), we then examined whether Gal7 could also translocate into ER microsomes 9 h following UV irradiation. We isolated a purified ER fraction from untreated and UV-irradiated cells to detect Gal7 by immunoblotting at the whole-cell level (WCE) and at the ER level (ER) (Figure 8C). We found that Gal7 does not constitutively localize to ER nor is it recruited to it following DNA damage (Figure 8C), reinforcing Gal7 selective recruitment to mitochondria.

We next addressed the question of how Gal7 and Bcl-2 interact under these stress conditions. Proteins were extracted to perform Bcl-2 IP using mitochondrial extracts and Bcl-2 antibodies, and the co-immunoprecipitated Gal7 amounts were evaluated by immunoblotting (Figure 8B, Bcl-2 IP). Interestingly, we have found that the amount of Gal7 bound to Bcl-2 was significantly reduced 9 h after UV irradiation when compared with untreated cells, indicating loss of Bcl-2/Gal7 interaction (Figure 8B). These results indicate that Gal7, endogenously associated to Bcl-2, is released upon apoptotic signal, probably to exert its pro-apoptotic function. Altogether, our findings imply that DNA damage induces Gal7 recruitment to the mitochondrial membrane but disrupts its interaction with Bcl-2.

DISCUSSION

In the present study, we aimed to extend current knowledge about the Bcl-2 interactome. We have used affinity purification followed by MS-based protein identification to further characterize Bcl-2 interacting proteins. To our knowledge, our data provide for the first time a global view of 127 Bcl-2–associated proteins in human colon cancer cells and of their various functional classifications. We have found many new potentially Bcl-2 interacting proteins that can be further validated through the use of immunocapture strategies.

Here, we focused on Gal7 that we have characterized as a novel mitochondrial Bcl-2 interactant in HCT116 colon carcinoma cells by co-IP using antibodies against Bcl-2. Endogenous constitutive Gal7/Bcl-2 association was confirmed by reciprocal co-IP using purified mitochondrial extracts and anti-Gal7 serum in several cell lines that express various amounts of the Gal7 protein. Pull-down assay

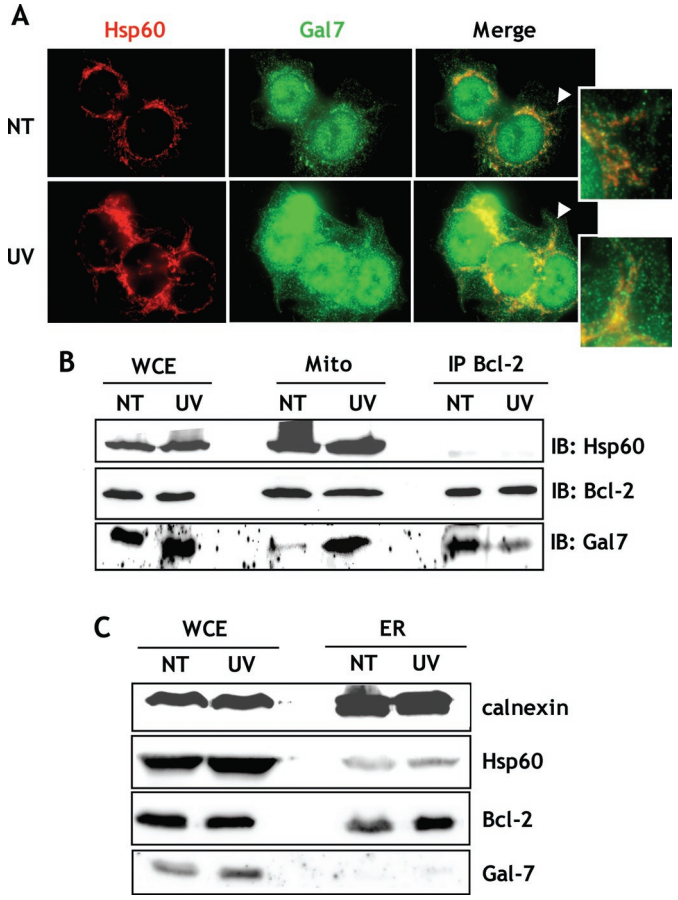

FIGURE 8: Disruption of Gal7-Bcl-2 interaction by UV irradiation. (A) Untreated (NT) and UV-exposed (UV) HCT116 cells were immunostained for 9 h after UV irradiation with anti-Gal7 antibody and anti-Hsp60 antibody (n = 3). For overlay, Hsp60 was assigned a red staining and Gal7 a green one. Images were analyzed using MetaMorph software. To compare the sensitivity of the signals, identical exposure time and intensity parameters were used for both treated and untreated cells. Bar = 5 μm. n = 3. (B) 9 h following UV exposure at 40 J/m^2, Bcl-2 was immunoprecipitated from purified mitochondria extracted from HCT116 cells using protein A–coated sepharose beads and anti-Bcl-2 antibody. The presence of Gal7 and Bcl-2 was analyzed by immunoblotting in total extracts (WCE), in mitochondrial extracts (Mito), and in immunoprecipitates (IP) (n = 2). NT: untreated cells. UV: UV-irradiated cells. (C) 9 h following UV irradiation at 40 J/m^2, ER fractions were isolated from HCT116 cells by differential centrifugation. The presence of Gal7 and Bcl-2 was analyzed by immunoblotting in total cell extracts (WCE) and in ER extracts (ER). Purity of the ER fraction obtained was assessed by detection of the ER-associated protein calnexin and of the mitochondrial protein Hsp60. NT: untreated cells. UV: UV-irradiated cells (n = 2).

experiments using purified proteins further confirmed that the interaction between Gal7 and Bcl-2 is direct. Thus, our results highlight the presence of a new Bcl-2/Gal7 complex at mitochondria and are consistent with a steady-state mitochondrial localization of Gal7 that we demonstrated by immunofluorescence analysis and immunoblotting using extracts obtained from purified mitochondria isolated on sucrose gradients. Bcl-2 is known to locate at the outer membrane of mitochondria (Chipuk and Green, 2008), inferring a similar localization pattern for Gal7. Gal7 has been shown to function extracellularly as a conventional lectin but has also been proposed to exert its pro-apoptotic effect intracellularly and was localized in the nucleus and the cytoplasm (Kuwabara *et al.*, 2002). This is the first report to identify a localization pattern specific to a subset of cytoplasmic Gal7. Although the specific mechanism by which Gal7 is constitutively localized to mitochondria needs to be clarified, our data clearly show that Bcl-2 participates in Gal7 targeting to mitochondria. Indeed, decreasing Bcl-2 expression using siRNA resulted in a significant reduction in Gal7 mitochondrial recruitment.

How could Gal7 interact with Bcl-2? It was previously reported that another lectin, galectin-3 (Gal3), can bind to Bcl-2 in vitro and exhibits an anti-apoptotic function (Yang *et al.*, 1996). Gal3, however, contains near its CRD the NWGR amino acid anti-death motif of the Bcl-2 protein family, suggesting that it could mimic the ability of the Bcl-2 family members to form heterodimers (Yang *et al.*, 1996). The Bcl-2/Gal3 interaction was shown to be lactose-inhibitable, probably due to the vicinity of CRD and NWGR motif in Gal3 (Akahani *et al.*, 1997). Because Gal7 does not contain any NWGR domain, and because our data have shown that the Bcl-2/Gal7 interaction is independent of lactose, we can assume that the Gal7 domain involved in Bcl-2 interaction is not closely located to its CRD. How Gal7 is precisely anchored to Bcl-2 remains to be specified.

What are the implications of Gal7 presence at mitochondria? One of the most plausible hypotheses is that Gal7 functions at mitochondria as a pro-apoptotic factor. Indeed, it has been shown that ectopic expression of Gal7 in HeLa and DLD-1 cancer cells renders them more sensitive to apoptosis induced by treatment with various apoptotic inducers (Kuwabara *et al.*, 2002). In this study, taking advantage of an apoptosis assay using intact mitochondria isolated from Gal7-overexpressing HeLa cells, we examined the ability of increased concentrations of endogenous Gal7 at mitochondria to release cytochrome *c* from mitochondria incubated with apoptotic inducers. Our findings clearly show that Gal7 overexpression at mitochondria promotes the release of mitochondrial intermembrane apoptogenic factors, such as cytochrome *c* and Smac/DIABLO following tBid or LND treatments. Thus, our data indicate that the presence of Gal7 at the mitochondrial membrane sensitizes the mitochondria to apoptotic stimuli. Direct incubation of intact mitochondria isolated from HeLa cells with recombinant Gal7 protein alone, however, did not induce the release of cytochrome *c* and SMAC/Diablo (unpublished data). This result strongly suggests that Gal7 is rather a weak pro-apoptotic protein targeting Bcl-2 and acts like a sensitizer that needs cooperation to induce potent killing during apoptosis.

It was already observed that during apoptosis Gal7 functions intracellularly and not extracellularly as a secreted or released protein (Kuwabara *et al.*, 2002). In this study, we report the specific mitochondrial localization of Gal7 in human cells. Our results strongly suggest that this mitochondrial localization of Gal7 is linked to its pro-apoptotic function. Therefore mitochondrial Gal7 is an interesting target for the control of cell survival following apoptotic stimuli, notably because our findings showed that it is further recruited to mitochondria following genotoxic stress. What could be the precise mechanism of action of Gal7 at mitochondria? Gal7 may act as a sensitizer such as Noxa or Bad (Zong *et al.*, 2001; Chen *et al.*, 2005), binding to anti-apoptotic proteins and then displacing the BH3-only proteins (termed activators), which become free to activate Bax/Bak and to induce mitochondrial permeabilization (Adams and Cory, 2007). Defining the affinity binding activity of Bcl-2 to Gal7 may help to evaluate this hypothesis. Alternatively, Gal7 may inhibit Bcl-2 activity by interacting with it, as p53, for example, which is known to inactivate Bcl-2 by binding to it (Tomita *et al.*, 2006). Gal7 binding to Bcl-2 may also change the tertiary structure of Bcl-2 and influence thereby the ability of Bcl-2 to interact with its partner proteins. Indeed, it was shown that Bcl-2 function can be regulated by Bcl-2

association with proteins not belonging to the Bcl-2 family. For example, it was observed that Bcl-2 is able to act as a "cell-killer" that triggers cytochrome *c* release and apoptosis upon binding to the nuclear orphan receptor Nur77 (Kolluri *et al.*, 2008). Finally, our findings may also indicate that Gal7 pro-apoptotic activity is constitutively inhibited by Bcl-2 and awaits a death signal to be released. Consistent with this hypothesis, we have found that the interaction of Gal7 with Bcl-2 occurs constitutively at mitochondria but is abolished following genotoxic stress such as UV light. These data indicate that the Gal7/Bcl-2 interaction is regulated upon apoptotic stimulus. UV irradiation may induce posttranslational modification of either Gal7 or Bcl-2 that promotes dissociation between the two proteins, or Gal7 may be released from Bcl-2 upon binding by BH3-only binding proteins to Bcl-2. Our findings suggest that, on dissociation between Gal7 and Bcl-2, Gal7 may act as a pro-apoptotic protein, leading to the initiation or the potentiation of the apoptotic cascade. Although further study is necessary to dissect the mitochondrial Gal7 function, our data indicate that the binding of Gal7 to Bcl-2 provides a new target for selectively enhancing the intrinsic apoptotic pathway.

MATERIALS AND METHODS

Cell culture and reagents

HCT116 and HeLa cells were obtained from the American Type Culture Collection and HaCaT cells from Cell Lines Services (Eppelheim, Heidelberg, Germany). Gal7-overexpressing HeLa cells, designated as HeLa-G7, and the corresponding parental HeLa cells, HeLa-v, were provided by Fu-Tong Liu (University of California, Sacramento) (Kuwabara *et al.*, 2002). All cells were maintained in DMEM supplemented with 10% fetal calf serum, 2 mM glutamine, penicillin at 50 U/ml and streptomycin at 50 μg/ml at 37°C in a humidified atmosphere containing 5% CO_2. The medium was supplemented with G418 at 0.3 mg/ml when HeLa-G7 and HeLa-v were concerned. Apoptosis was induced by exposing cells to UV-C light at the given doses through phosphate-buffered saline (PBS) using a UV cross-linker (Appligene Oncor, Illkirch, France). After UV irradiation, fresh medium was added to the cells, which were grown for the indicated periods. Both detached and attached cells were collected and combined for the subsequent analysis.

LND was purchased from Sigma (St. Louis, MO). Recombinant Bcl-2 and tBid were a gift from J.C. Martinou (University of Geneva, Geneva, Switzerland), and recombinant Gal7 was purchased from R&D Systems (Minneapolis, MN). The following antibodies were used for immunoblotting and IP: monoclonal anti-Bcl-2 antibody (clone 124; Dako Corp., Copenhagen, Denmark), polyclonal anti-Bcl-2 antibody (DC21; Santa Cruz Biotechnology, Santa Cruz, CA), anti-Gal7 serum (obtained as described; Magnaldo *et al.*, 1998), monoclonal anti-Hsp60 antibody (clone LK2; Sigma), monoclonal anti-Gal7 antibody (Bethyl Laboratories, Montgomery, TX), monoclonal anti-actin (Mab1501; Millipore Corp., Billerica, MA), polyclonal anti-Gadd34 (S-20; Santa Cruz Biotechnology), polyclonal anti-Estrogen Receptor (Santa Cruz Biotechnology), monoclonal anti-calnexin (clone 37; BD Transduction Laboratories, Franklin Lakes, NJ), monoclonal anti-PCNA (clone PC-10; Santa Cruz Biotechnology), polyclonal anti–cytochrome *c* (SC-7159; Santa Cruz Biotechnology), polyclonal anti–cleaved caspase-3 (5A1E; Cell Signaling Technology, Danvers, MA), polyclonal anti-PARP (9542; Cell Signaling Technology), and polyclonal anti-Smac/DIABLO (S-0941; Sigma).

Mitochondria isolation and mitochondrial proteins solubilization

Cells were seeded at a density of 200 cells/mm^2 and grown for 24 h before being exposed to UV light or treated with drugs when specified. Cells were then collected, washed with ice-cold PBS, and centrifuged for 8 min at 1200 × *g* at 4°C. Cellular pellets were resuspended in 1 ml of mannitol buffer (MB; 10 mM HEPES, pH 7.5, 210 mM mannitol, 70 mM sucrose, 0.1 mM ethylene glycol tetraacetic acid [EGTA]) per 30 million cells containing proteases and phosphatase inhibitors (Roche, Basel, Switzerland) and then homogenized with a Dounce glass homogenizer. The homogenate was centrifuged at 500 × *g* for 10 min to remove unbroken cells, and the resulting supernatant was then centrifuged at 2000 × *g* for 15 min to pellet nuclei. After a last centrifugation at 15,000 × *g* for 15 min, a heavy membrane fraction (HM) enriched in mitochondria was obtained in the pellet and washed with MB. To obtain highly pure mitochondrial fractions required for MS experiments, we added a density gradient purification step following the differential centrifugations as previously described (Estaquier and Arnoult, 2007). Briefly, the enriched mitochondrial fraction was resuspended in a minimal volume of MB containing proteases and phosphatase inhibitors and was loaded onto a discontinuous sucrose gradient consisting of a layer of 16 ml of a solution of 1.2 M sucrose, 10 mM HEPES, pH 7.5, 0.1 mM EGTA, and 0.1% bovine serum albumin (BSA) on top of a layer of 19 ml of a solution of 1.6 sucrose, 10 mM HEPES, pH 7.5, 0.1 mM EGTA, and 0.1% BSA. After centrifugation at 27000 rpm in a Beckman SW28 rotor for 2 h at 4°C, pure mitochondria were collected at the interface of the 1.2 and 1.6 M sucrose solution layers and washed with MB. Mitochondrial proteins were solubilized by incubating the pellet of mitochondria with a solution of 750 mM diaminocaproic acid, 50 mM Bis-Tris, pH 7, 0.1 mM EGTA, and 2% CHAPS supplemented with phosphatases and protease inhibitors during 1 h on ice, with regular vortexing and by subsequent sonication for 20 s. The purity of the mitochondrial protein fraction (IM) obtained was evaluated by assessing the removal of nonmitochondrial proteins by immunoblotting.

ER microsome preparation

Cells were grown for 24 h before being exposed to UV light or left untreated. Cells were then collected, washed with ice-cold PBS and centrifuged for 5 min at 600 × *g* at 4°C. Cellular pellets were resuspended in Isotonic Extraction Buffer (IEB: 10 mM HEPES, pH 7.9, 250 mM sucrose, 25 mM KCl, 1 mM EGTA) containing proteases inhibitors (Roche) and then homogenized with a Dounce glass homogenizer. The homogenate was centrifuged at 1000 × *g* for 10 min at 4°C to pellet nuclei. The resultant supernatant was centrifuged at 12,000 × *g* for 15 min at 4°C. The resultant intermediate postmitochondrial fraction was centrifuged for 60 min at 100,000 × *g* at 4°C. Pellets containing the microsomal ER fraction were analyzed by immunoblotting.

IP

Mitochondrial proteins (500 μg to 1 mg) were precleared with Sepharose-conjugated protein A or G in IP buffer (IB) containing 50 mM Tris, pH 7.5, 150 mM NaCl, and 0.1 mM EDTA supplemented with phosphatases and protease inhibitors. They were then incubated overnight at 4°C with either a pool of monoclonal anti–Bcl-2 antibody (4 μg/mg), polyclonal anti–Bcl-2 antibody (2.7 μg/mg), and Sepharose-conjugated protein G beads or anti-Gal7 serum (1:50 [vol/vol]) and Sepharose-conjugated protein A beads, with constant shaking. Control IPs were performed using isotype-matched nonrelevant anti-Estrogen Receptor, anti-actin, or anti-Gadd34 antibodies (IP IgG). Beads were then centrifuged at 1600 × *g* for 2 min and washed three times with IB. Immunoprecipitated proteins were separated on a 12% SDS–PAGE gel and analyzed by MS or by Western blotting as described further.

In-gel tryptic digestion of mitochondrial proteins, identification of proteins by nano-liquid chromatography–electrospray ionization LTQ-Orbitrap MS/MS analysis, and database searching

Following protein separation by SDS–PAGE and Coomassie Blue staining, bands were excised from the gel and washed first in 100 mM ammonium bicarbonate for 15 min at 37°C, and then in 100 mM ammonium bicarbonate/acetonitrile (ACN) (1:1 [vol/vol]) for 15 min at 37°C. Cystein reduction and alkylation were performed by successive incubations in solutions of 10 mM dithiothreitol, 100 mM NH_4HCO_3 for 35 min at 56°C and 55 mM iodoacetamide, 100 mM NH_4HCO_3 for 30 min at room temperature in the dark, respectively. In-gel tryptic digestion was then performed as described previously (Bouyssie *et al.*, 2007) with minor modifications. Briefly, after several washing steps to eliminate the stain, gel pieces were dried under a vacuum to be rehydrated in a sufficient covering volume (50–75 µl) of modified trypsin solution (20 ng/µl in 25 mM NH_4HCO_3; Promega, Madison, WI) for 15 min in an ice bath. Trypsin digestion was performed overnight at 37°C under shaking. Peptides were extracted three times at 37°C for 15 min under shaking, using 50 mM NH_4HCO_3 (once) and 5% formic acid (twice) in 50% ACN. The peptide mixture was dried under vacuum and stored at –20°C.

For MS analysis, tryptic peptides were resuspended with 12 µl of 5% ACN/0.05% trifluoroacetic acid and were submitted to nano-liquid chromatography MS/MS using an Ultimate3000 system (Dionex Corp., Sunnyvale, CA) coupled to an electrospray ionization LTQ-Orbitrap mass spectrometer (Thermo Fisher Scientific, Bremen, Germany) operating in positive mode with a spray voltage of 1.4 kV. Five ml of each sample was loaded on a C18 precolumn (300 µm internal diameter (ID) × 5 mm; Dionex) at 20 µl/min. After 5-min desalting, the precolumn was switched online with the analytical column (75 µm ID × 15 cm PepMap C18; Dionex) equilibrated in 95% solvent A (5% ACN, 0.2% formic acid [FA]) and 5% solvent B (80% ACN, 0.2% FA). Peptides were eluted using a 5–50% gradient of solvent B for 80 min at 300 nl/min flow rate. Data were acquired with Xcalibur (LTQ-Orbitrap Software, version 2.2 beta 5; Thermo Fisher Scientific). The mass spectrometer, externally calibrated, was operated in the data-dependent acquisition mode to automatically switch between Orbitrap-MS and LTQ-MS/MS (MS2) acquisition. Survey MS scans were acquired in the Orbitrap on the 300–2000 m/z range with the resolution set to a value of 60,000 at m/z 400. Up to five of the most intense multiply charged ions (2+ and 3+) per scan were fragmented by collision-induced dissociation (CID) in the linear ion trap. A dynamic exclusion window was applied within 60 s. All tandem mass spectra were collected using normalized collision energy of 35%, an isolation window of 4 m/z, and 1 microscan. Other instrumental parameters included maximum injection times and automatic gain control (AGC) targets of 250 ms and 500,000 ions, respectively, for the Fourier transform MS (FTMS), and 100 ms and 10,000 ions, respectively, for LTQ MS/MS. Data were analyzed using Xcalibur software (version 2.0 SR2; Thermo Fisher Scientific), and MS/MS centroid peak lists were generated using the extract_msn.exe executable (Thermo Fisher Scientific) integrated into the Mascot Daemon software (Mascot version 2.2.1; Matrix Science, Boston, MA). The following parameters were set to create the peak lists: parent ions in the mass range 400–4500, no grouping of MS/MS scans, threshold at 1000. A peak list was created for each fraction analyzed (i.e., gel band), and individual Mascot searches were performed for each fraction.

Data were searched using Mascot server (Mascot version 2.2.01; Matrix Science) against Homo Sapiens sequences in the Swiss-Prot TrEMBL database (68,579 sequences). This database consists of UniProtKB/Swiss-Prot Protein Knowledgebase Release 53.1 merged in-house with UniProtKB/TrEMBL Protein Database Release 36.1. Carbamidomethylation of cysteine was set as a fixed modification, and oxidation of methionine was set as a variable modification for all MASCOT searches. The mass tolerances in MS and MS/MS were set to 5 ppm and 0.8 Da, respectively, and the instrument setting was specified as "ESI Trap." Trypsin was designated as the protease (the specificity was set for cleavage after K or R); up to two missed cleavages were allowed. Protein hits were automatically validated if they satisfied one of the following criteria: identification with at least one top ranking peptide (bold and red) with a Mascot score of more than 50 ($p < 0.001$); at least two top ranking peptides each with a Mascot score of more than 35 ($p < 0.05$); or at least three top ranking peptides each with a Mascot score of more than 30 ($p < 0.1$), as determined by the Mascot Search program and using the automatic validation module of our in-house–developed software MFPaQ (version 4.0.0) (Bouyssie *et al.*, 2007). Proteins identified with a single peptide were confirmed by manual inspection of the MS/MS spectra. From all the validated result files corresponding to the fractions of a one-dimensional gel lane, MFPaQ was used to generate a unique, nonredundant list of proteins, by comparing proteins or protein groups (composed of all the protein sequences matching the same set of peptides) according to accession numbers and by creating clusters from protein groups found in different gel slices if they have one common member. Protein list comparisons were based on the comparison of protein groups (hits matching the same set of peptides) from different lists, and the MFPaQ software assigned these protein groups as "shared" or "specific," depending on whether they have common members.

To evaluate false-positive rates, all the initial database searches were performed using the "decoy" option of Mascot, in other words, the data were searched against a combined database containing the real specified protein sequences (target database, Swiss-Prot TrEMBL human) and the corresponding reversed protein sequences (decoy database). MFPaQ used the same criteria to validate decoy and target hits, calculated the false discovery rate [FDR = number of validated decoy hits / (number of validated target hits + number of validated decoy hits) × 100] for each gel band analyzed, and calculated the average of FDR for all bands belonging to the same gel lane (i.e., to the same sample). Results were considered to be relevant if the false-positive rate never exceeded 1%.

Gene ontology and data mining

Data analysis of the protein list was performed using the DAVID bioinformatics resource that allows extracting a gene functional classification associated with protein lists. The percentage of enriched specific proteins from our list was assessed with a threshold for statistical significance <0.001.

Predicted protein–protein interaction analysis was performed using STRING. STRING retrieves known and predicted protein–protein interactions that have been defined using different methods such as experiments, gene neighborhood, data mining, and coexpression. A network map was created with default settings, allowing for experimentally verified and predicted interactions.

Immunoblotting

Proteins boiled for 5 min in Laemmli buffer were resolved by 12% SDS–PAGE and transferred to nitrocellulose membranes. The membranes were blocked with Tris-buffered saline (TBS)-T (10 mM Tris, pH 8, 150 mM NaCl, 0.05% Tween 20) containing 5% nonfat dry milk for 1 h at room temperature and incubated overnight at 4°C with

primary antibodies. For equal loading control, immunoblots were also probed with monoclonal anti-Hsp60 antibody that recognizes a mitochondrial matrix protein. Membranes were then incubated with horseradish peroxidase–conjugated secondary antibodies (Cell Signaling Technology). After extensive washes with TBS-T, proteins were visualized using an ECL+ protein detection system (Pierce, Rockford, IL).

Immunofluorescence

Cells were seeded onto coverslips at a density of 200 cells/mm^2 and grown for 24 h. They were then fixed with 3.7% formaldehyde in PBS for 15 min, permeabilized with 0.25% Triton in PBS for 10 min, and incubated with 3% BSA in PBS for 1 h. Coverslips were incubated with anti-Gal7 serum (1:50) and monoclonal anti-Hsp60 antibody (1:50 [vol/vol]) at room temperature for 1 h each. After extensive washes with PBS, coverslips were incubated for 1 h at room temperature with FITC-conjugated goat anti-rabbit or Alexa 594–conjugated goat anti-mouse antibodies (Molecular Probes, Carlsbad, CA). Image acquisition was performed using a DM600 microscope (Leica Microsystems, Wetzlar, Germany) fitted with a Roper COOLsnap ES CCD camera (Roper Scientific GmbH, Ottobrunn, Germany). Images were denoised using the Nearest Neighbours approach of the two-dimensional Deconvolution setup of MetaMorph software (filter size: 2; scaling factor: 0.5; result scale: 2). For blocked antibody control, the diluted rabbit antibody was preincubated with a 10-fold molar excess of the immunogenic protein for 2 h at room temperature before applying to the coverslip.

GST-Gal7 pull-down assay

The pGEX-2T-1A12 vector expressing a GST-Gal7 fusion protein was described previously (Magnaldo *et al.*, 1995), and the parental pGEX2T'6 vector containing a GST tag was purchased from GE Healthcare (GE Healthcare Europe, Orsay, France). Both vectors were transformed into *Escherichia coli* BL21(DE3) RIPL bacterial strain (Stratagene, La Jolla, CA). The transformed bacteria were grown in L-Broth medium containing ampicillin at 100 μg/ml with the addition of 100 μM isopropyl beta-D-thiogalactoside to induce GST-fusion protein expression. The bacteria were then harvested and lysed by sonication in PBS containing 1% Triton and lysozyme at 10 μg/ml. Lysates were centrifuged at 12,000 × *g* for 30 min, and GST-fusion proteins were purified by incubating equal amount of lysates containing either GST alone, or the GST-Gal7 fusion proteins with gluthatione-sepharose 4B beads (GE Healthcare), 50% slurry, for 3 h at room temperature with constant shaking.

For pull-down reactions, 25 μl of GST or Gal7-GST beads were incubated overnight at room temperature with 0.1 μg of recombinant Bcl-2 in a final volume of 1 ml of PBS containing 1% Triton and protease inhibitors. When mentioned, 20 or 100 mM lactose was incubated along with the recombinant proteins. The beads were washed six times with PBS containing protease inhibitors, boiled in Laemmli loading buffer, and analyzed by SDS–PAGE/immunoblotting. The bound Bcl-2 protein was detected using monoclonal anti-Bcl-2 antibody. The relative intensity of the Bcl-2 bands was quantified using ImageJ software (National Institutes of Health).

siRNA transfection

HeLa-Gal7 and HeLa parental cells were transfected with pooled sequences of siRNA targeting Bcl-2 or nonspecific scramble siRNA duplexes (Dharmacon, Thermo Fisher Scientific, Lafayette, CO) using Lipofectamine 2000 reagent according to the manufacturer's instructions (Invitrogen). The final concentration of siRNA was 100 nM. 48 h after transfection of siRNA, cells were harvested for mitochondria isolation, whole-cell extract preparation for immunoblotting analysis, or immunofluorescence analysis as described further.

Apoptosis assay using isolated mitochondria

Mitochondria were isolated from HeLa-Gal7 and HeLa-v cells and incubated according to a standard protocol (Scorrano *et al.*, 2002; Baricault *et al.*, 2007). Briefly, mitochondria were isolated by differential centrifugation at 4°C in 0.2 M sucrose, 10 mM Tris-MOPS [3-(N-morpholino)propanesulfonic acid], pH 7.4, 0.1 mM EGTA. Pelleted mitochondrial fractions (0.5 mg/ml) were incubated for 20 min at 25°C in 125 mM KCl, 10 mM Tris-MOPS, pH 7.4, 1 mM Pi, 5 mM glutamate, 10 μM EGTA with 16 nM tBid or 25 μM LND as indicated. After incubation, mitochondrial fractions were pelleted by centrifugation at 15,000 × *g* for 10 min at 4°C. The supernatant was kept for analysis, and the mitochondrial fractions were resuspended in the same volume of Laemmli sample buffer. Equivalent volumes containing 10 μg of cytosolic or pelleted mitochondrial proteins were run on SDS–PAGE and processed for immunoblotting.

ACKNOWLEDGMENTS

We thank Fu-Tong Liu for the Gal7-overexpressing HeLa cells, Jean-Claude Martinou for recombinant Bcl-2 and tBid proteins, Chahine Ledra for technical assistance, and Françoise Alquier and Robert Mercurey for helpful comments. This work was funded by the Centre National de la Recherche Scientifique (CNRS), by the University of Toulouse, and by GlaxoSmithKline. Christelle Villeneuve and Ludovic Canelle were recipients of postdoctoral fellowships from GlaxoSmithKline Oncology.

REFERENCES

Adams JM, Cory S (2007). The Bcl-2 apoptotic switch in cancer development and therapy. Oncogene 26, 1324–1337.

Akahani S, Nangia-Makker P, Inohara H, Kim HR, Raz A (1997). Galectin-3: a novel antiapoptotic molecule with a functional BH1 (NWGR) domain of Bcl-2 family. Cancer Res 57, 5272–5276.

Antonsson B (2001). Bax and other pro-apoptotic Bcl-2 family "killer-proteins" and their victim the mitochondrion. Cell Tissue Res 306, 347–361.

Baricault L, Segui B, Guegand L, Olichon A, Valette A, Larminat F, Lenaers G (2007). OPA1 cleavage depends on decreased mitochondrial ATP level and bivalent metals. Exp Cell Res 313, 3800–3808.

Bernerd F, Sarasin A, Magnaldo T (1999). Galectin-7 overexpression is associated with the apoptotic process in UVB-induced sunburn keratinocytes. Proc Natl Acad Sci USA 96, 11329–11334.

Bouyssie D, Gonzalez de Peredo A, Mouton E, Albigot R, Roussel L, Ortega N, Cayrol C, Burlet-Schiltz O, Girard JP, Monsarrat B (2007). Mascot file parsing and quantification (MFPaQ), a new software to parse, validate, and quantify proteomics data generated by ICAT and SILAC mass spectrometric analyses: application to the proteomics study of membrane proteins from primary human endothelial cells. Mol Cell Proteomics 6, 1621–1637.

Boyd JM, Malstrom S, Subramanian T, Venkatesh LK, Schaeper U, Elangovan B, D'Sa-Eipper C, Chinnadurai G (1994). Adenovirus E1B 19 kDa and Bcl-2 proteins interact with a common set of cellular proteins. Cell 79, 341–351.

Brunelle JK, Letai A (2009). Control of mitochondrial apoptosis by the Bcl-2 family. J Cell Sci 122, 437–441.

Cao Z, Said N, Amin S, Wu HK, Bruce A, Garate M, Hsu DK, Kuwabara I, Liu FT, Panjwani N (2002). Galectins-3 and -7, but not galectin-1, play a role in reepithelialization of wounds. J Biol Chem 277, 42299–42305.

Chen L, Willis SN, Wei A, Smith BJ, Fletcher JI, Hinds MG, Colman PM, Day CL, Adams JM, Huang DC (2005). Differential targeting of prosurvival Bcl-2 proteins by their BH3-only ligands allows complementary apoptotic function. Mol Cell 17, 393–403.

Chipuk JE, Green DR (2008). How do BCL-2 proteins induce mitochondrial outer membrane permeabilization? Trends Cell Biol 18, 157–164.

Chipuk JE, Kuwana T, Bouchier-Hayes L, Droin NM, Newmeyer DD, Schuler M, Green DR (2004). Direct activation of Bax by p53 mediates mitochondrial membrane permeabilization and apoptosis. Science 303, 1010–1014.

Cory S, Adams JM (2002). The Bcl2 family: regulators of the cellular life-or-death switch. Nat Rev Cancer 2, 647–656.
Erin N, Bronson SK, Billingsley ML (2003). Calcium-dependent interaction of calcineurin with Bcl-2 in neuronal tissue. Neuroscience 117, 541–555.
Estaquier J, Arnoult D (2007). Inhibiting Drp1-mediated mitochondrial fission selectively prevents the release of cytochrome c during apoptosis. Cell Death Differ 14, 1086–1094.
Gendronneau G, Sidhu SS, Delacour D, Dang T, Calonne C, Houzelstein D, Magnaldo T, Poirier F (2008). Galectin-7 in the control of epidermal homeostasis after injury. Mol Biol Cell 19, 5541–5549.
Kolluri SK *et al.* (2008). A short Nur77-derived peptide converts Bcl-2 from a protector to a killer. Cancer Cell 14, 285–298.
Kuwabara I, Kuwabara Y, Yang RY, Schuler M, Green DR, Zuraw BL, Hsu DK, Liu FT (2002). Galectin-7 (PIG1) exhibits pro-apoptotic function through JNK activation and mitochondrial cytochrome c release. J Biol Chem 277, 3487–3497.
Lithgow T, van Driel R, Bertram JF, Strasser A (1994). The protein product of the oncogene bcl-2 is a component of the nuclear envelope, the endoplasmic reticulum, and the outer mitochondrial membrane. Cell Growth Differ 5, 411–417.
Luo X, Budihardjo I, Zou H, Slaughter C, Wang X (1998). Bid, a Bcl2 interacting protein, mediates cytochrome c release from mitochondria in response to activation of cell surface death receptors. Cell 94, 481–490.
Magnaldo T, Bernerd F, Darmon M (1995). Galectin-7, a human 14-kDa S-lectin, specifically expressed in keratinocytes and sensitive to retinoic acid. Dev Biol 168, 259–271.
Magnaldo T, Fowlis D, Darmon M (1998). Galectin-7, a marker of all types of stratified epithelia. Differentiation 63, 159–168.
Mahajan NP, Linder K, Berry G, Gordon GW, Heim R, Herman B (1998). Bcl-2 and Bax interactions in mitochondria probed with green fluorescent protein and fluorescence resonance energy transfer. Nat Biotechnol 16, 547–552.
Nakahara S, Raz A (2006). On the role of galectins in signal transduction. Methods Enzymol 417, 273–289.
Ng FW, Nguyen M, Kwan T, Branton PE, Nicholson DW, Cromlish JA, Shore GC (1997). p28 Bap31, a Bcl-2/Bcl-XL- and procaspase-8-associated protein in the endoplasmic reticulum. J Cell Biol 139, 327–338.
Polyak K, Xia Y, Zweier JL, Kinzler KW, Vogelstein B (1997). A model for p53-induced apoptosis. Nature 389, 300–305.
Rapoport EM, Kurmyshkina OV, Bovin NV (2008). Mammalian galectins: structure, carbohydrate specificity, and functions. Biochemistry (Mosc) 73, 393–405.
Rebollo A, Perez-Sala D, Martinez AC (1999). Bcl-2 differentially targets K-, N-, and H-Ras to mitochondria in IL-2 supplemented or deprived cells: implications in prevention of apoptosis. Oncogene 18, 4930–4939.
Scorrano L, Ashiya M, Buttle K, Weiler S, Oakes SA, Mannella CA, Korsmeyer SJ (2002). A distinct pathway remodels mitochondrial cristae and mobilizes cytochrome c during apoptosis. Dev Cell 2, 55–67.
Sheibani N, Tang Y, Sorenson CM (2008). Paxillin's LD4 motif interacts with bcl-2. J Cell Physiol 214, 655–661.
Shimizu S, Narita M, Tsujimoto Y (1999). Bcl-2 family proteins regulate the release of apoptogenic cytochrome c by the mitochondrial channel VDAC. Nature 399, 483–487.
Tomita Y, Marchenko N, Erster S, Nemajerova A, Dehner A, Klein C, Pan H, Kessler H, Pancoska P, Moll UM (2006). WT p53, but not tumor-derived mutants, bind to Bcl2 via the DNA binding domain and induce mitochondrial permeabilization. J Biol Chem 281, 8600–8606.
Tsujimoto Y, Croce CM (1986). Analysis of the structure, transcripts, and protein products of bcl-2, the gene involved in human follicular lymphoma. Proc Natl Acad Sci USA 83, 5214–5218.
Yang E, Zha J, Jockel J, Boise LH, Thompson CB, Korsmeyer SJ (1995). Bad, a heterodimeric partner for Bcl-XL and Bcl-2, displaces Bax and promotes cell death. Cell 80, 285–291.
Yang RY, Hsu DK, Liu FT (1996). Expression of galectin-3 modulates T-cell growth and apoptosis. Proc Natl Acad Sci USA 93, 6737–6742.
Yang RY, Liu FT (2003). Galectins in cell growth and apoptosis. Cell Mol Life Sci 60, 267–276.
Yu J, Zhang L, Hwang PM, Kinzler KW, Vogelstein B (2001). PUMA induces the rapid apoptosis of colorectal cancer cells. Mol Cell 7, 673–682.
Zong WX, Lindsten T, Ross AJ, MacGregor GR, Thompson CB (2001). BH3-only proteins that bind pro-survival Bcl-2 family members fail to induce apoptosis in the absence of Bax and Bak. Genes Dev 15, 1481–1486.